

Heat capacity of CH₄ on graphite and the quantum cell model

Kathleen A. Hunzicker and James M. Phillips

Department of Physics, University of Missouri—Kansas City, Kansas City, Missouri 64110

(Received 23 June 1986)

We present a discussion about calculated heat capacities for physisorbed systems based on a quantum-mechanical cell model. Recent calculations on monolayers have shown the lateral contribution to the heat capacity to be below the classical harmonic limit as the temperature is increased to near the triple line. We interpret this effect to be due to the increasing anharmonic nature of the potential. The effect is enhanced by the expansion of the lattice. New results for the methane-on-graphite system are given and compared to the experiments of Marx and Wassermann. Comparisons to classical Monte Carlo simulations show that the quantum cell theory gives good results for the equilibrium lattice constant, internal energy, and the heat capacity for the midrange of temperatures. As a limit of the quantum cell theory, the quantum corrected cell model is much more efficient in the middle- and high-temperature range.

I. INTRODUCTION

Heat-capacity measurements have contributed greatly to the understanding of adsorbate phases.¹⁻⁹ Primarily, the observation of heat-capacity peaks has been used to study phase transitions. The emphasis in this discussion is, however, on the approach to the harmonic classical limit as the temperature increases nearer to the triple line. Recent experiments¹⁰ with CH₄ on graphite are in agreement with the unusual behavior found in our calculations here and previously^{11,12} (see Fig. 1). Namely, the heat capacity does not approach the classical harmonic limit.

This report discusses calculated heat capacities based on a quantum-mechanical cell model for physisorbed systems. We believe our results show the extent of anharmonicity in the interactions of these systems.

An understanding of the high-temperature behavior of the calculated heat capacity of a solid monolayer by any model is important for at least two reasons. First, does

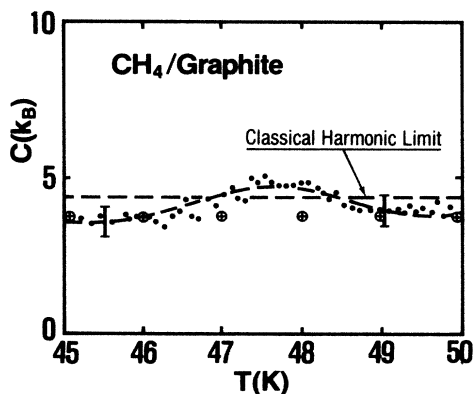


FIG. 1. A comparison of the heat capacity for a monolayer of methane on graphite calculated, \oplus , by QCT with the experimental data, \bullet , of Marx and Wasserman (Ref. 10). Note, the maximum in the experimental data is due to the C-IC transition and should be ignored in this comparison.

the model [in this case quantum cell theory (QCT)] sufficiently account for heat capacity in this region? This near universal problem is well illustrated by Klein *et al.*¹³ Second, if the model (QCT) is able to reasonably predict the high-temperature heat capacity, does the approach to the classical limit give a measure of the anharmonicity of the adsorbate interactions?¹⁴

II. CALCULATIONS

In previous papers, Phillips and Bruch¹¹ and Phillips¹² found broad maxima in the heat capacity of certain two-dimensional (2D) solids as calculated by the non-self-consistent quantum cell model. In this paper, we attempt to explain the origins of the apparent maximum in the heat capacity for monolayers of argon (2D), xenon (2D), and methane [three-dimensional (3D)] by the quantum

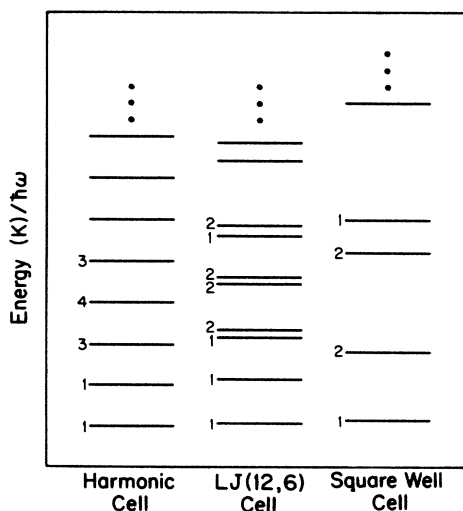


FIG. 2. A diagram of the lowest-energy eigenvalues for three of the cell potential models. The numbers on the side are the degeneracies.

cell model and for real maximum from a (2D) square-well calculation. The relevance to methane on graphite experiments will be discussed in a later section.

The quantum cell model is a good approximation for a class of 2D solids over a broad range of temperatures.^{11,12,15,16} Any departure of the calculated heat capacities of this model from harmonic theory is of interest. In this discussion, we use the results of four quantum cell models with parameters¹¹ representative of monolayer solids on smooth substrates. The cell potential $\omega(r)$ (Ref. 16) is assumed to be: (1) a harmonic (Einstein) model, (2) a cylindrical square well, (3) a circularly averaged potential of 36 shells of Lennard-Jones LJ(12,6) interacting atoms in a 2D triangular lattice,¹⁷ and (4) a 3D calculation for a methane monolayer on graphite.¹⁸ The first and second cell potentials represent the harmonic-approximation reference system and an extreme anharmonic case. The third^{11,15} is a more realistic anharmonic system. The fourth case is described later in this section.

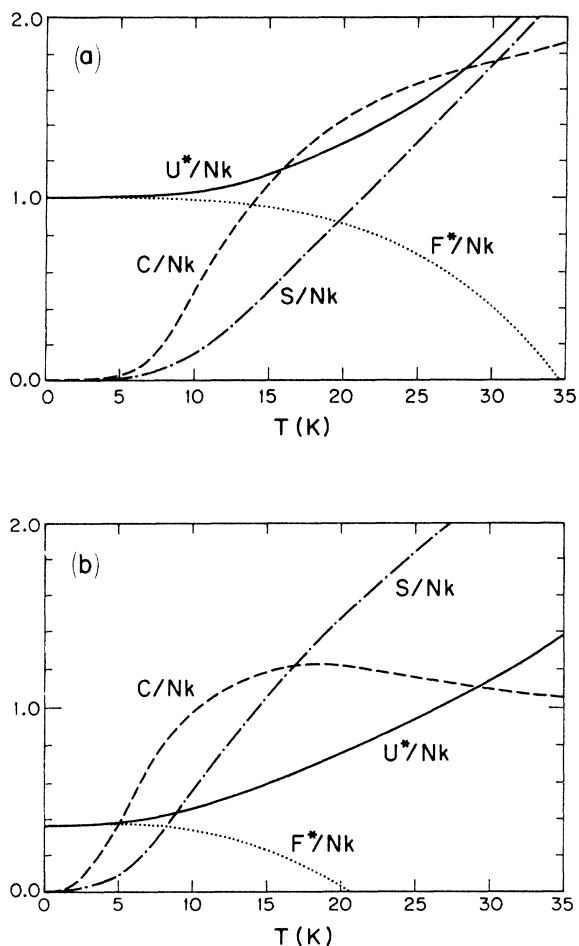


FIG. 3. A summary of the quantum cell results for the thermodynamic properties of a 2D triangular lattice of atoms with argon parameters. (a) is from the harmonic model results and (b) the square-well model. The results were taken along the sublimation line ($\phi=0$) as defined by the full LJ(12,6) of Ref. 11 with argon parameters. The data shows an inflection point in S/Nk_B .

TABLE I. Heat capacity of a methane monolayer on graphite at zero spreading pressure. These results do not include the contribution due to the rotation of the methane molecules. The number of significant figures represents the computational precision not the physical accuracy. The model represents a scaling of a Lennard-Jones system to methane parameters. The heats (Ref. 18) of formation of monolayer and bilayer structures are within 5% of the experimental values. The columns are the lateral (in plane) contribution C_{xy} , the vertical degree of freedom contribution C_z , and the total heat capacity for the system.

T (K)	C_{xy}/Nk_B	C_z/Nk_B	C_{tot}/Nk_B
5	0.001 90	0.000 00	0.001 90
10	0.183 96	0.000 56	0.184 52
15	0.616 43	0.016 33	0.632 76
20	0.991 97	0.074 75	1.066 72
25	1.249 39	0.170 12	1.419 51
30	1.401 94	0.279 21	1.681 15
35	1.492 06	0.385 20	1.877 26
40	1.541 95	0.480 53	2.022 47
45	1.562 51	0.563 25	2.125 76
50	1.560 74	0.634 03	2.194 77
55	1.537 29	0.694 42	2.231 71
60	1.485 23	0.746 13	2.231 36

The quantum cell approximation accurately accounts for the anharmonicity but omits correlations and the accompanying communal entropy.^{19,20} Comparisons of the quantum cell model to quasiharmonic lattice dynamics^{11,15} show the relative importance of anharmonicity and correlations. Some of the lost communal entropy can be recovered.²⁰ Barker²¹ has given a classical self-consistent cell model.

We solve the radial form of the 2D Schrödinger equation

$$-(\hbar^2/2M)\nabla^2\psi + \omega(r) = E_{n,l}$$

for the energy eigenvalues $E_{n,l}$ of the three $\omega(r)$ cell potentials. The integers n and l are the energy and angular momentum quantum numbers, respectively, and M is the mass of the atom in the cell. The relative magnitudes and degeneracies of the energy eigenvalues are shown in Fig.

TABLE II. Heat capacity of a methane monolayer on graphite for fixed-lattice constant. Features are the same as those in Table I.

T (K)	C_{xy}/Nk_B	C_z/Nk_B	C_{tot}/Nk_B
5	0.001 21	0.000 00	0.001 21
10	0.153 48	0.000 56	0.154 04
15	0.551 07	0.016 33	0.567 40
20	0.911 17	0.074 75	0.985 92
25	1.158 89	0.170 12	1.329 00
30	1.319 86	0.279 21	1.599 07
35	1.424 82	0.385 20	1.810 02
40	1.494 54	0.480 53	1.975 07
45	1.541 77	0.563 25	2.105 02
50	1.574 26	0.634 03	2.208 30
55	1.596 85	0.694 42	2.291 27
60	1.612 57	0.746 13	2.358 70

TABLE III. A comparison of heat capacity, internal energy, and equilibrium lattice constant for a 2D LJ(12,6) system with argon parameters. All results were taken on the sublimation curve defined by a minimum in the Helmholtz free energy (zero spreading pressure) as calculated by QCT. The results of the classical cell model are in the CCM column, quantum cell theory (QCT), and quantum-corrected cell model (QCCM). The Monte Carlo results scaled to argon parameters are the following: $T = 15.6$ K, $C/Nk_B = 1.91$, $U/Nk_B = -372.8895$; $T = 31.25$ K, $C/Nk_B = 1.76$, $U/Nk_B = -337.3568$; $T = 46.88$ K, $C/Nk_B = 1.78$, $U/Nk_B = -295.3070$; $T = 50.33$ K, $C/Nk_B = 1.71$, $U/Nk_B = -284.7646$.

T (k)	$L_0(\text{\AA})$		U/Nk_B		C_A/Nk_B		
	QCT	CCM	QCCM	QCT	CCM	QCCM	QCT
20.0	3.87	-360.387	-346.511	-345.886	1.88		1.30
30.0	3.89	-337.739	-331.897	-328.809	1.82	1.77	1.57
40.0	3.94	-312.996	-309.672	-306.919	1.76	1.75	1.64
45.0	3.96	-299.572	-296.992	-294.957	1.72	1.73	1.64
50.0	3.99	-285.156	-283.148	-281.332	1.69	1.69	1.62
55.0	4.03	-269.427	-267.876	-266.015	1.64	1.65	1.58

2. The first two models are solved analytically but the third and fourth models are studied by the numerical methods outlined in Ref. 11 and 18.

The thermodynamic properties are obtained by substituting the energy eigenvalues $E_{n,l}$ into the partition function and its derivatives. The thermal properties of the harmonic model are also given in Fig. 3 to be compared to the harmonic model. Note that the results show a maximum in the heat capacity. The thermal properties of the LJ(12,6) cell potential are given in Ref. 11 for neon and argon parameters.

In the harmonic model the spring constant is defined by the LJ(12,6) argon parameters to be $\kappa(T) = \frac{1}{2} \sum_{i,j} \nabla^2 \phi(r_{ij})$. In the square-well cell model, the cell radius is defined as $a^2 = (2\sqrt{3}/\pi)^{1/2} (L - \sigma)^2$ where L is the lattice constant and σ is the root of the LJ(12,6) potential for argon.

The 3D calculation for the monolayer of methane-on-graphite system was also modeled as a quantum cell prob-

lem. In this case, the Schrödinger equation was written for a cylindrically symmetric cell potential. The lateral interactions for the adsorbate molecules are LJ(12,6) potentials scaled to methane parameters¹² ($\epsilon/k_B = 137$ K and $\sigma = 3.6914$ Å). Substrate mediated interactions²² via the MacLachlan formula²³ were included. The lateral contribution from the periodic potential of the graphite was taken to be the Fourier series representation by Steele.²⁴ Vertical contributions to the cell potential are from the Steele $\Sigma(4-10)$ potential.²⁵ The parameters for the potentials were determined in a previous paper.¹² The energy eigenvalues of this system are used in the partition function to determine the thermodynamic properties.

The detailed heat-capacity results for the methane on graphite (3D) calculation are given in Tables I and II. The results in Table I are taken along the monolayer sublimation line defined by a constant spreading pressure ($\phi = 0$). The results in Table II are taken at a constant lattice dilation ($L = 4.26$ Å, the $\sqrt{3} \times \sqrt{3}$ registry configura-

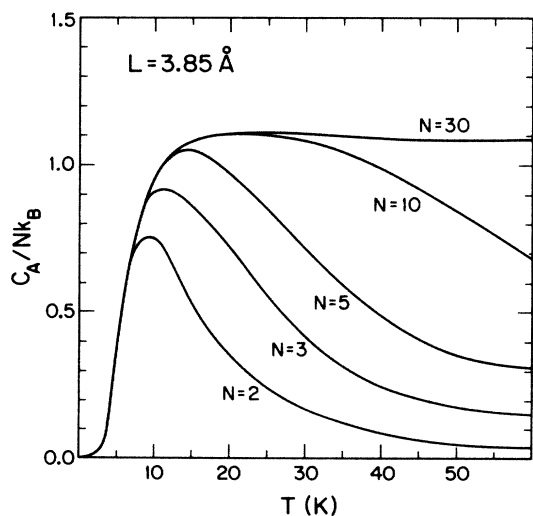


FIG. 4. A diagram of the heat capacity at constant area with temperature from the square-well cell model showing a real maximum at lower temperatures. The number of square-well states (Fig. 2) included is increased from 2 to 100 (agrees with 30 levels result).

TABLE IV. Heat capacity of a 2D Lennard-Jones system with argon parameters by quasiharmonic lattice dynamics and quantum cell theory for a fixed-lattice constant. The lattice constant is that of the uncompressed lattice at 5 K (3.8511 Å). The QHT data follows the T^2 law quite well up through 3 K. The calculations were done in the QHT case by the numerical second derivative of the Helmholtz free energy.

T (K)	C_A/Nk_B	
	QHT	QCT
1	0.0059	
2	0.0243	
3	0.0568	
4	0.1069	
5	0.1767	0.0175
6	0.2643	
10	0.6903	0.4337
15	1.1400	0.9423
20	1.4237	1.2569
25	1.5962	1.4351
30	1.7046	1.5384

tion). The spreading pressure increases considerably as the temperature rises.

III. ANHARMONICITY AND HEAT CAPACITY

There are several physical effects which could potentially cause the heat capacity of a solid to approach its classical limit from above as the temperature increases to the triple line.

One possibility is for a system with a small number of allowed energy levels, e.g., a two-state system, the upper state can become saturated as the temperature rises reducing the derivative of the internal energy with temperature to zero. Figure 4 shows the results from the square-well model at a fixed-lattice constant and an increasing number of energy levels included in the statistical mechanics. The curve stabilizes for $N=30$ energy quantum levels and does not change further even for $N=100$. This would suggest that the very anharmonic nature of the potential is more the cause of the heat-capacity maximum

than the number of levels which enter into the problem.

Another real possibility for the effect is the simple failure of the quantum cell model to properly account for the anharmonic nature of the system. Cell models differ from harmonic theories of lattice dynamics in just this way. The QCT model is tested for a system with sizable quantum contributions, i.e., argon [see Tables III and IV and Figs. 3(b), 5, and 6], for nearly classical systems we have used, previously the quantum-corrected cell model (QCCM).¹⁵ The QCCM theory is an attempt to include quantum effects into the classical cell model (CCM). Quantum-mechanical corrections are introduced into the partition function of the CCM by a formal expansion in powers of \hbar^2 . Using the Wigner-Kirkwood expansion,¹⁵ the 2D partition can be written

$$Z_N = \text{Tr}(-H/k_B T) \\ \simeq (Mk_B T/2\pi\hbar^2)^N Q'(N, A, T)^N,$$

where

$$Q'(N, A, T) = 2\pi \int_0^\infty d\rho \rho \exp[-(\rho)/k_B T] \{1 - \hbar^2/[12M(k_B T)^2] \{ \nabla^2 \omega(\rho) - 1/(2k_B T) [\nabla \omega(\rho)]^2 \} + O(\hbar^4) \}.$$

For a classical system, xenon results of QCT are compared to Monte Carlo simulation, classical cell, and quantum-corrected cell (see Tables V and VI). Our conclusion is that QCT fully accounts for anharmonicity.¹¹ For argon parameters, the heat capacity for a 3D crystal is well predicted by an early version of the quantum cell idea (see Fig. 13 of Ref. 13, also Ref. 26).

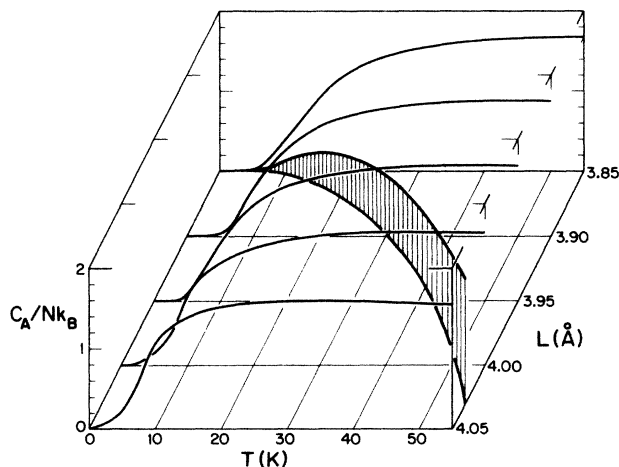


FIG. 5. A diagram of the heat capacity at constant area with temperature for a range of lattice constants. The results are for the full LJ(12,6) cell model of Ref. 11. The shaded contour is for the sublimation line (zero spreading pressure $\phi=0$). The projection of this contour onto a plane is the graph of Fig. 2 in Ref. 11 which has the apparent maximum at approximately 45 K. There is a slight dip in the data for 55–60 K in all models, this is near or beyond the triple-point melting temperature.

In 2D, quantum cell for a LJ(12,6) system with xenon parameters results can be compared to the classical Monte Carlo simulations.²⁷ Table III gives new results for the xenon system with the earlier work on the quantum-corrected cell model, and Monte Carlo simulations. As can be seen in Table III, the predictions for the equilibrium lattice constant, and internal energy are rather close in the proper range of 30–60 K for all three methods. The low-temperature results are in good agreement with quasiharmonic lattice dynamics.^{15,27} The quantum-corrected cell model results for heat capacity are quite close to the simulations from 30 K to the triple line. The Monte Carlo (MC) calculation must be done at sufficiently high temperatures to overcome the lack of zero-point

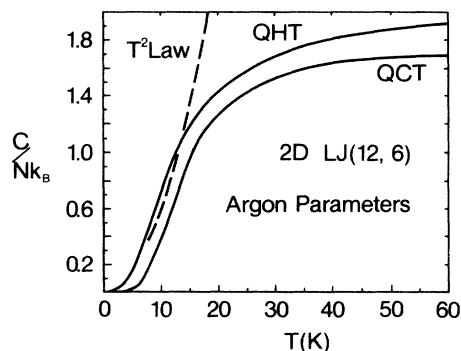


FIG. 6. A comparison of the heat capacities calculated by quasiharmonic theory (QHT) and quantum cell theory (QCT) for a two-dimensional triangular lattice of LJ(12,6) interaction particles with argon parameters. The calculations were all carried out at the equilibrium lattice constant at 5 K, $L_0=3.8511$ Å. Below 3 K the QHT results fit the T^2 law quite well.

TABLE V. A comparison of heat capacity, internal energy, and equilibrium lattice constant for a 2D LJ(12,6) system with xenon parameters. All of the results have been taken on the sublimation curve defined by a minimum in the Helmholtz free energy (zero spreading pressure). Above 60 K the QCT calculation was very inefficient. The number of quantum levels required for convergence to the QCCM limit was very large. The results of Monte Carlo simulations are in the MC column, classical cell model (CCM), quantum cell theory (QCT), and quantum-corrected cell model (QCCM).

T (K)	L_0 (Å)				U/Nk_B^a				C_A/Nk_B^b			
	MC	CCM	QCT	QCCM	MC	CCM	QCT	QCCM	MC	CCM	QCT	QCCM
30.0	4.51	4.51	4.51	4.51 ^c	-3.1126	-3.1107	-3.0903	-3.0972	1.91	1.92	1.77	1.88
60.0	4.57	4.57	4.57	4.57	-2.816	-2.8192	-2.8135	-2.8144	1.86	1.83	1.69	1.83
90.0	4.67	4.67		4.66	-2.465	-2.4681		-2.4660	1.75	1.72		1.72
96.6	4.70	4.70		4.69	-2.377	-2.3777		-2.3968	1.71	1.69		1.69

^aThe units are reduced, to get kelvin units multiply by 230.

^bThe heat capacity results by Monte Carlo simulation were rerun for long (15 000 moves per molecule) tests. The results differ slightly from those in Ref. 11.

^cThe prediction for 30 K using quasiharmonic lattice dynamics (QHT), is 4.51 Å and the energy is 1%T below the QCT value. At 5 K, the QHT lattice constants are identical and the energy agrees to within 0.2%.

effects. At 30 K, the heat-capacity results of the two methods (QCCM and MC) are approaching each other and both drift downward for increasing temperature. Near the triple line, the quantum cell theory is very inefficient. The angular momentum quantum number must exceed $l = 12$ and the radial levels $n = 50$. The number of grid separations for the Richardson extrapolation to determine the eigenvalues for the $l = 0$ states (see Ref. 11) must be increased fourfold. Even using the plane-wave methods of Ref. 11, the computational effort is near that of the Monte Carlo simulations. The QCCM calculation is at least 10^3 faster.

The downward drift of the heat capacity with temperature is present in all of the uncompressed monolayer calculations and the Monte Carlo simulations except for neon [Fig. 3(a)]. Neon is quite quantum mechanical in 2D (Ref. 16) and its triple line is comparatively quite low. Melting simply preempts the effect in neon.

A good test of these models to experiments²⁸ is for the xenon monolayer on the (111) surface of silver with substrate-mediated forces included (see Table VI). The comparisons of the thermal expansion and a number of thermodynamic properties, including heats,²⁹ with the experiments of Webb and co-workers is quite good. With all of these cross checks of the models and methods we believe the dropping of the heat capacity near the triple line is physical and the primary origin is the anharmonicity. As discussed in Ref. 11, the most important correction to the harmonic Hamiltonian for most of these monolayer

systems is the approximation for the anharmonicity.

In Fig. 5 (argon parameters), the heat capacity for fixed-lattice dilation (C_A) does not show a maximum before the triple line. However, the approach to the classical limit is successively lower for each curve with increasing lattice dilation. So, when the heat capacity is plotted along the sublimation line there appears to be a maximum. The same is true for the methane-on-graphite system (Tables I and II). For the cases of xenon and the square well the maximum persists even for fixed-lattice parameters. A generalization can be drawn empirically that the more anharmonic and expanded the system becomes the more pronounced effect.

This type of behavior is reasonable in the light of the equipartition of energy theorem for nonquadratic systems. A quantum-mechanical system in its classical limit with a power-law interaction potential $V(x) = c|x^n|$ has a thermal average $\langle V \rangle$ which approaches $(1/n + 1/2)k_B T$.¹⁴ The square-well potential, as an extreme anharmonic example, approaches the classical limit $\frac{1}{2}k_B T$ instead of $k_B T$ per degree of freedom. Figure 4 illustrates the point for the 2D square-well potential. The internal energy is all kinetic.

The quantum cell model appears to account very well for the increasing anharmonicity of the monolayer systems with increasing temperature. It is consistent at the lower temperatures with lattice dynamics, the functional limit as $T \rightarrow 0$ notwithstanding,³¹ and verifiable for mid-range temperatures by computer simulation. The quan-

TABLE VI. The Monte Carlo results for heat capacity, internal energy, equilibrium lattice constant, pressure, and bulk modulus for a Xe/Ag(111) monolayer system along the sublimation line. The interaction model is described in Refs. 15 and 31. All of the results were taken on the sublimation curve defined by a minimum in the Helmholtz free energy (zero spreading pressure). Experimental comparisons for the system are give in Ref. 30.

T (K)	L_0 (Å)	C_A/Nk_B	$U/Nk_B T$	$P/\rho k_B T$	$B_t/\rho k_B T$
30.0	4.45	1.93	-19.9513	0.0160	374.69
50.0	4.49	1.94	-11.0656	0.0363	174.24
80.0	4.57	1.82	-5.9578	-0.0050	62.76
90.0	4.62	1.74	-4.9383	0.0644	36.10

tum cell model comes into question however when the system is about to melt. The xenon case makes the point. The 2D LJ(12,6) system with xenon parameters has a relatively high triple line at approximately 95 K.^{27,32} The system is quite classical at the higher temperatures so the quantum cell calculations and computer simulations should both be able to account for the anharmonic contributions to the thermal properties. In the computer simulations a record was made of the structure of the monolayer by graphics plots of the atom positions. The appearance of defect pairs, voids, and the number of nearest neighbors not equal to six, corresponds to the QCT heat capacity falling below the simulation values. Even though the predicted thermal expansion and internal energies are close, the fluctuations in the internal energy from the simulation (heat capacity) are larger than those from the quantum cell calculation. The quantum cell model, as we have applied it,¹¹ would appear to represent the role of anharmonicity in physisorbed systems rather well but does not allow for the additional localized excitations. The Holian harmonic correction²⁰ does not apply directly to this issue.

The most important comparison resulting from this study is the good agreement between the QCT predictions for the heat capacity of a monolayer of methane on graphite and the measurements of Marx and Wassermann.¹⁰ In Fig. 1, we have attempted to reproduce their data plot (Fig. 2 of Ref. 10). We have superimposed our QCT results on their graph. Some of their data points are missing in our drawing. When our calculated values overlapped the data points we omitted them for clarity of the figure.

Two features of Fig. 1 are important: first, the agreement between theory and experiment, and second, the fact that the data is at a high-temperature limit of $\frac{7}{2}k_B$ instead of the classical harmonic limit of $\frac{9}{2}k_B$. Also, note the bump in the experimental data due to the commensurate-incommensurate (C-IC) transition has been constrained out of the calculation. Our prediction of this C-IC transition has been published.²⁹ The rotational contribution of $\frac{3}{2}k_B$ has been added directly to values like those given in Table II for the reported temperatures. A full analysis of the rotational contribution is given by Hamilton.³³ In the 45–50 K range of temperature, the rotational contribution is slightly above $\frac{3}{2}k_B$ (Ref. 33) which would give an even better agreement than that shown in Fig. 1.

We observe that the data of Marx and Wassermann and our calculations both fall $1k_B$ below the conventional value and the error bars indicate the result can be taken as physical. This agreement with experiment, Monte Carlo simulation, and the other calculation methods leads us to the conclusion that anharmonicity in monolayer systems is significant and measurable.

IV. SUMMARY

We have attempted to show that the low maxima in the heat capacities of monolayer solids are a physical result.

Also, that the effect is not a limitation of QCT or the computational methodologies. We suggest the physical origins of the downward drift in the heat capacity, as the temperature approaches the triple line, is due to the increasingly anharmonic nature of the expanding lattice. As can be seen from the equipartition of energy theorem for power-law potentials, $|x^n|$ with $n > 2$, in the high-temperature limit, has the energy going to $(1/n + \frac{1}{2})k_B T$. Therefore the heat capacities should fall below the harmonic limit of $(\frac{1}{2} + \frac{1}{2})k_B T$ per degree of freedom. Except for 2D-neon LJ(12,6), all of the monolayer systems studied: (1) 2D-argon LJ(12,6), (2) 2D-xenon LJ(12,6), (3) 2D Xe/Ag(111) full model (4) 2D square-well, and (5) 3D methane-on-graphite, all show the anharmonic influence in the high-temperature heat capacity along their solid-vapor equilibrium lines. The extent of the drop in the heat capacity with increasing temperature can quite possibly be a measure of the degree of anharmonicity present in the system. We have also run the Monte Carlo simulations for LJ(6,3) potential (it is more harmonic at the same temperatures). The heat capacity from these simulations approaches the classical harmonic limit in the same fashion as the harmonic approximation curve (QHT) of Fig. 6.

It is also important to note that the systems we have studied cover the range of quantum-mechanical effects from neon to the quite classical xenon at the higher temperatures. Quantum cell theory would appear to reasonably predict the thermodynamic properties of these systems over the middle to high range of the stable solid. However, the quantum corrected cell model is much more efficient for the middle and high range of temperatures in the very classical xenon case. In principle, the difference between the cell theory predictions and the computer simulations for the heat capacity are due to two effects, a missing piece of the communal entropy and contributions from additional collective excitations.

The variety of system types and the several computational methods we have used, all confirm each other in the appropriate conditions where any two or more combinations apply. The close agreement of quasiharmonic lattice dynamics,¹⁵ at low temperatures, and quantum-corrected cell model and Monte Carlo simulations,²⁷ at middle and high temperatures, with Xe/Ag(111) experiments³⁰ gives a realistic basis to the models and methods. The close comparisons with the experimental data of Marx and Wassermann¹⁰ QCT give a physical result and indicate that the role of anharmonicity in the lateral interactions of monolayer systems is significant.

ACKNOWLEDGMENTS

We wish to thank Professor L. W. Bruch, Professor M. H. W. Chan, and Professor J. G. Dash for helpful discussions. Acknowledgment is made to the donors of the Petroleum Research Fund, administered by the American Chemical Society, for the support of this research.

- ¹J. G. Dash, *Films on Solid Surfaces* (Academic, New York, 1975); G. B. Huff and J. G. Dash, *J. Low. Temp. Phys.* **24**, 155 (1976); T. T. Chung and J. G. Dash, *Surf. Sci.* **66**, 559 (1977); J. G. Dash and J. Ruvalds, *Phase Transitions in Surface Films* (Plenum, New York, 1980); F. C. Motteler and J. G. Dash, *Phys. Rev. B* **31**, 346 (1985).
- ²M. Bretz and J. G. Dash, *Phys. Rev. Lett.* **26**, 963 (1971); M. Bretz, J. G. Dash, D. C. Hickernell, E. O. McLean, and O. E. Vilches, *Phys. Rev. A* **8**, 1589 (1973); **9**, 2814 (1974).
- ³D. C. Hickernell, E. O. McLean, and O. E. Vilches, *Phys. Rev. Lett.* **28**, 789 (1972).
- ⁴R. L. Elgin and D. L. Goodstein, *Phys. Rev. A* **9**, 2657 (1974).
- ⁵R. Marx and R. Brown, *Solid State Commun.* **33**, 229 (1980).
- ⁶D. M. Butler, J. A. Litzinger, G. A. Stewart, and R. B. Griffiths, *Phys. Rev. Lett.* **42**, 1289 (1979).
- ⁷W. A. Steele and R. Karl, *J. Colloid Interface Sci.* **28**, 397 (1968).
- ⁸A. A. Antoniou, *J. Chem. Phys.* **64**, 4901 (1976).
- ⁹M. H. W. Chan, A. D. Migone, K. D. Miner, and A. R. Li, *Phys. Rev. B* **30**, 2681 (1984); Q. M. Zhang, H. K. Kim, and M. H. W. Chan, *ibid.* **33**, 413 (1986).
- ¹⁰R. Marx and E. F. Wassermann, *Surf. Sci.* **117**, 267 (1982).
- ¹¹J. M. Phillips and L. W. Bruch, *J. Chem. Phys.* **79**, 6282 (1983).
- ¹²J. M. Phillips, *Phys. Rev. B* **29**, 5865 (1984).
- ¹³M. L. Klein, G. K. Horton, and J. L. Feldman, *Phys. Rev.* **184**, 968 (1969).
- ¹⁴R. P. Bell, *Proc. R. Soc. (London)* **183**, 328 (1945).
- ¹⁵J. M. Phillips and L. W. Bruch, *Surf. Sci.* **81**, 109 (1979); L. W. Bruch and J. M. Phillips, *ibid.* **91**, 1 (1980); and the references therein.
- ¹⁶L. W. Bruch and J. M. Phillips, *J. Phys. Chem.* **86**, 1146 (1982).
- ¹⁷J. A. Barker, *Lattice Theories of the Liquid State* (Pergamon, New York, 1963).
- ¹⁸J. M. Phillips, *Phys. Rev. B* **34**, 2823 (1986).
- ¹⁹J. O. Hirschfelder, C. F. Curtiss, and R. B. Bird, *Molecular Theory of Gases and Liquids* (Wiley, New York, 1954).
- ²⁰B. L. Holian, *Phys. Rev. B* **22**, 1394 (1980).
- ²¹J. A. Barker, *J. Chem. Phys.* **44**, 4212 (1966); J. A. Barker and E. R. Cowley, *ibid.* **73**, 3452 (1980).
- ²²L. W. Bruch, *Surf. Sci.* **125**, 194 (1983).
- ²³A. D. MacLachlan, *Mol. Phys.* **7**, 381 (1964).
- ²⁴W. A. Steele, *The Interaction of Gases with Solid Surfaces* (Pergamon, New York, 1974).
- ²⁵W. A. Steele, *J. Chem. Phys.* **82**, 617 (1978).
- ²⁶I. J. Zucker, *Philos. Mag.* **3**, 987 (1958).
- ²⁷J. M. Phillips, L. W. Bruch, and R. D. Murphy, *J. Chem. Phys.* **75**, 5097 (1981).
- ²⁸J. M. Phillips and L. W. Bruch, *J. Chem. Phys.* **83**, 3660 (1985).
- ²⁹J. M. Phillips, *Phys. Rev. B* **29**, 5865; **29**, 5859 (1984).
- ³⁰J. Unguris, L. W. Bruch, E. R. Moog, and M. B. Webb, *Surf. Sci.* **87**, 415 (1979); P. I. Cohen, J. Unguris, and M. B. Webb, *ibid.* **58**, 429 (1976); L. W. Bruch, P. I. Cohen, and M. B. Webb, *ibid.* **59**, 1 (1976).
- ³¹R. Kubo, *Statistical Mechanics* (North-Holland, Amsterdam, 1971).
- ³²J. A. Barker, D. Henderson, and F. F. Abraham, *Physica (Utrecht) A* **106**, 226 (1981).
- ³³J. J. Hamilton, Ph.D. thesis, California Institute of Technology, 1983.